

# Supporting Information

## Magnetically sensitive radical photochemistry of non-natural flavoproteins

Tilo M. Zollitsch,<sup>1</sup> Lauren E. Jarocho,<sup>1</sup> Chris Bialas,<sup>2</sup> Kevin B. Henbest,<sup>3</sup> Goutham Kodali,<sup>2</sup> P. Leslie Dutton,<sup>2</sup> Christopher C. Moser,<sup>2</sup> Christiane R. Timmel,<sup>\*3</sup> P. J. Hore,<sup>\*1</sup> and Stuart R. Mackenzie,<sup>\*1</sup>

<sup>1</sup>Department of Chemistry, University of Oxford, Physical and Theoretical Chemistry Laboratory, OX1 3QZ, United Kingdom

<sup>2</sup>Johnson Research Foundation, Department of Biochemistry and Biophysics, University of Pennsylvania, Philadelphia, PA 19104, U.S.A.

<sup>3</sup>Department of Chemistry, University of Oxford, Centre for Advanced Electron Spin Resonance, Inorganic Chemistry Laboratory, OX1 3QR, United Kingdom

\* Corresponding authors:

Christiane.Timmel@chem.ox.ac.uk

Peter.Hore@chem.ox.ac.uk

Stuart.Mackenzie@chem.ox.ac.uk

## 1. Temporal deconvolution of ring-down traces

In cavity ring-down spectroscopy (CRDS), the intensity of probe light leaving an optical cavity is measured alternately with ( $I(t)$ ) and without ( $I'(t)$ ) a pump pulse as a function of the time,  $t$ , after the probe pulse. Following Brown *et al.*,<sup>1</sup>  $I(t)$  and  $I'(t)$  are given by

$$I(t) = I(0) \exp \left[ -\frac{2.3026c}{L} \int_0^t \alpha(t') dt' - \frac{t}{\tau_0} \right] \quad (1)$$

$$I'(t) = I(0) \exp \left[ -\frac{t}{\tau_0} \right], \quad (2)$$

where  $L$  is the length of the cavity,  $c$  is the speed of light,  $\tau_0$  is the ring-down time in the absence of a pump pulse, and  $\alpha(t)$ , the change in the absorbance of the sample as a result of the pump pulse, is proportional to the change in the absorber concentration,  $\Delta[A](t)$ . It follows from equation (1) that the ring-down time of the light leaving the cavity is independent of  $t$  for a sample with constant absorbance. However, the changing concentrations of reactants, intermediates, and products following the pump pulse mean that, in general, the absorbance will vary as a function of  $t$ . In this work the change in absorbance during the cavity ring-down was approximated by

$$\alpha(t) = \beta e^{-kt} + \gamma, \quad (3)$$

where  $\beta$  and  $\gamma$  are constant during the measurement of the ring-down (typically a few microseconds) and  $k$  is a rate constant. Using a least-squares routine (The MathWorks, MATLAB R2014b), the ratio  $I(t)/I'(t)$  was fit to  $f(t)$ , where

$$f(t) = \exp \left[ -\frac{2.3026c}{L} \frac{\beta}{k} (1 - e^{-kt}) - \frac{2.3026c}{L} \gamma t \right], \quad (4)$$

in order to determine values for  $\beta$ ,  $\gamma$  and  $k$ .  $\Delta[A](0)$ , at the start of the ring-down period, was then obtained from the differential absorbance at  $t = 0$ ,  $\alpha(0) = \beta + \gamma$ .

## 2. Spectral analysis

### (a) Control maquette – characterization of the $^3F^*$ spectrum

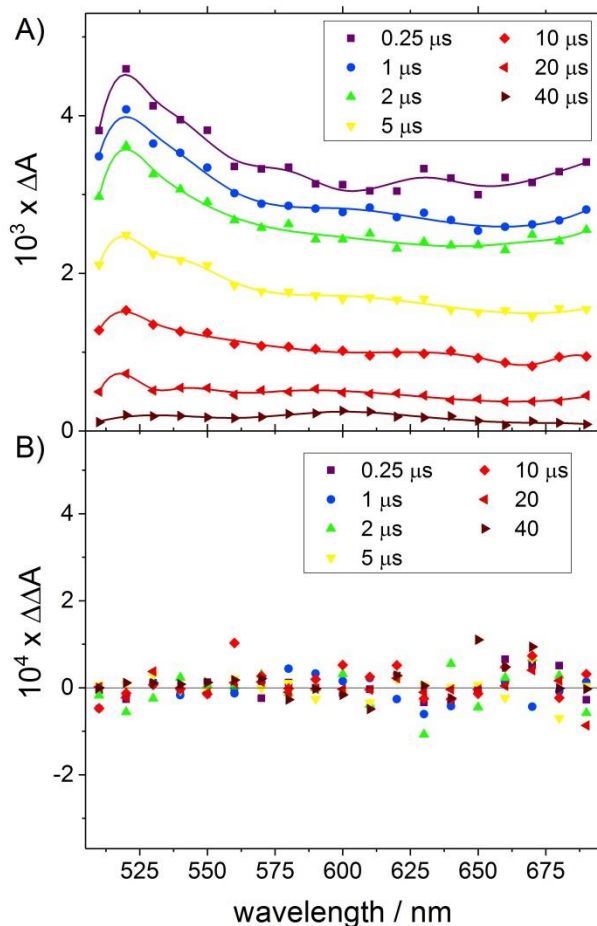


**Figure S1.** (A) Differential absorbance spectra,  $\Delta A$ , and (B) action spectra,  $\Delta\Delta A$ (30 mT) (defined in equation (1) in the main text), for the control maquette (*ca.* 20  $\mu$ M) in pH 6.5 phosphate buffer at various PPD times. The  $\Delta\Delta A$  data show that there is no detectable magnetic field effect for the control maquette.

The  $\Delta A$  spectra of the control maquette in Figure S1A show a broad, featureless absorption in the wavelength range 520-690 nm, assigned to the excited triplet state of the flavin,  $^3F^*$ . The sharp drop in  $\Delta A$  from 520 nm to 510 nm marks the onset of the flavin ground-state absorption. Unlike the tryptophan-containing maquettes, the control does not show a prominent  $FH^\bullet$  band peaking at *ca.* 600 nm, confirming that the excited flavin is not reduced by electron transfer from a nearby amino acid. However, the residual absorption observed at  $t = 20 \mu$ s and 40  $\mu$ s resembles

that of  $\text{FH}^\bullet$ .<sup>2</sup> This signal arises from a neutral flavin radical,  $(\text{FH}^\bullet)^\dagger$ , produced during the photodegradation of the flavin. Structurally similar to  $\text{FH}^\bullet$ ,  $(\text{FH}^\bullet)^\dagger$  is hypothesized to form by proton-coupled electron transfer from the ribityl group of the riboflavin to the isoalloxazine ring and reacts to give the stable photodegradation product, lumichrome,<sup>3</sup> identified from a UV/visible spectrum of the control sample recorded after the CRDS and other photochemical measurements (Supporting Information in Ref. <sup>4</sup>). Significantly less lumichrome accumulated during the CRDS measurements on the Trp- and His- containing maquettes because of the competing electron transfer reactions.

The  $\Delta\Delta A$  data in Figure S1B show that no magnetic field effect could be detected for the control maquette at any wavelength or PPD time. This is consistent with the absence of magnetically sensitive radical pairs when there is no electron-donating amino acid residue available to reduce the triplet flavin.

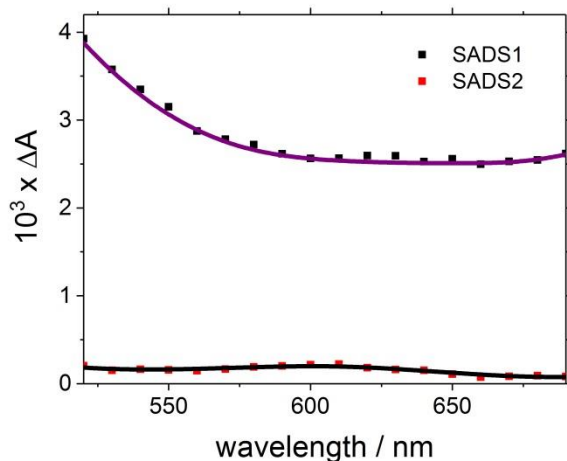
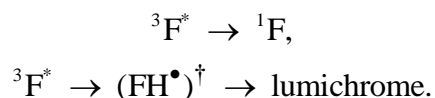


**Figure S2.** Species associated difference spectrum (SADS) of  $^3\text{F}^*$  (black squares) and  $(\text{FH}^\bullet)^\dagger$  (red squares) estimated by global analysis of the  $\Delta A$  spectra of the control flavomaquette. The solid lines are spline interpolations.

The time- and wavelength-resolved data in Figure S1A for the control maquette were analyzed using global target analysis based on the kinetic model:



The species-associated decay spectra (SADS1 and SADS2), shown in Figure S2, are similar to previously reported absorption spectra of  $^3\text{F}^*$  and  $\text{FH}^\bullet$ , respectively.<sup>2,5,6</sup> SADS1 was therefore assigned to  $^3\text{F}^*$  and used in the spectral deconvolution described in the main text and in more detail below. SADS2 is assigned to  $(\text{FH}^\bullet)^\dagger$  but was not used for further analysis.

(b) Characterization of the  $\text{FH}^\bullet$  spectrum using the histidine maquette, H6

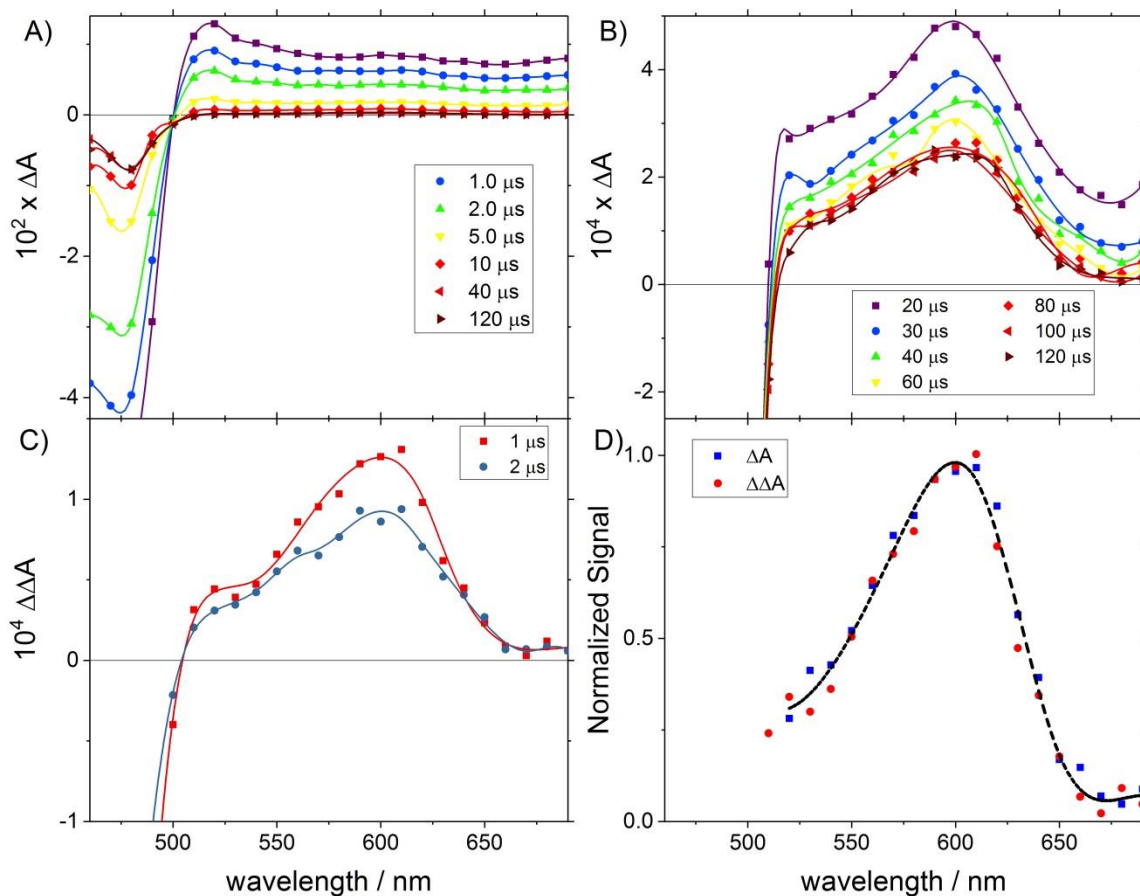


**Figure S3.**  $\Delta A$  spectra of *ca.* 20  $\mu\text{M}$  H6 maquette in pH 6.5 phosphate buffer taken at various PPD times with a focus on (A) early (1–40  $\mu\text{s}$ ) and (B) late times (20–120  $\mu\text{s}$ ). Note the different scales for  $\Delta A$  in (A) and (B). (C)  $\Delta\Delta A$  spectra of *ca.* 20  $\mu\text{M}$  H6 in pH 6.5 phosphate buffer taken at  $t = 1$  and 2  $\mu\text{s}$ . Solid lines are spline fits to guide the eye. (D) Comparison of the  $\Delta A$  spectrum of H6 recorded at  $t = 100 \mu\text{s}$  (blue squares) with the  $\Delta\Delta A$  spectrum recorded at 1  $\mu\text{s}$  (red circles). The interpolated average is shown as a dashed black line.

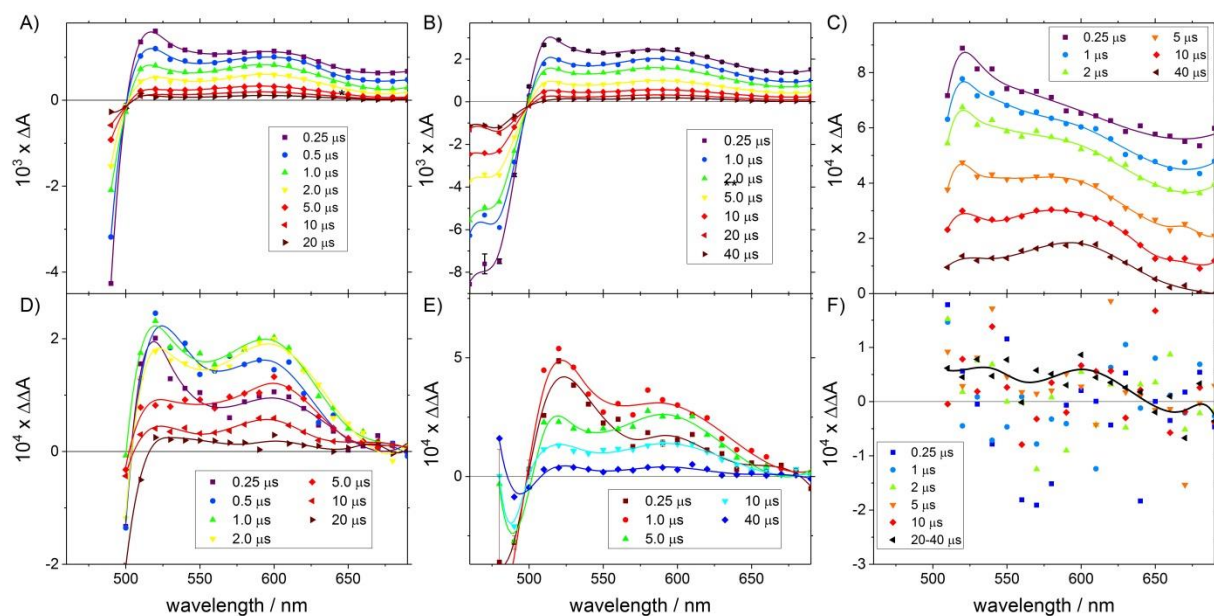
Histidine undergoes a hydrogen atom transfer reaction with excited flavins.<sup>7</sup> This alternative mechanism for formation of a radical pair leads directly to the formation of a FH• radical. As such, a maquette (designated H6) devoid of tryptophan but with a single histidine (His) at position 6 on helix 2 was used to obtain the reference spectrum of FH• shown in Figure 4A in the main text. Figure S3A shows  $\Delta A$  spectra of H6 measured at various PPD times. As in the case of the control and the Trp-containing maquettes, the bleaching of the flavin ground state was observed as a negative contribution to  $\Delta A$  at wavelengths below 520 nm. Between 520 and 640 nm the absorption is dominated by  $^3F^*$ , FH•, and/or  $F^{\bullet-}$ , while only  $^3F^*$  absorbs significantly beyond 650 nm. The  $\Delta A$  signal at 680 nm, which decays exponentially within the first 20  $\mu s$  with a lifetime of  $2.3 \pm 0.1 \mu s$ , is attributed to the disappearance of  $^3F^*$ . The spectrum observed between 80 and 120  $\mu s$  shows no further decay (Figure S3B) and closely resembles that of FH•.<sup>2</sup> As histidine readily reduces flavins to form neutral radical pairs of the form [FH• His•],<sup>8,9</sup> and because His radicals do not absorb significantly in the visible region, the absorption band at PPD times  $\geq 80 \mu s$  was assigned to FH•.

The magnetic field action spectra,  $\Delta\Delta A$ , recorded at  $t = 1$  and 2  $\mu s$  are identical in shape to the  $\Delta A$  spectrum of FH• (see Figures S3C and D), consistent with the formation of a spin-correlated flavin-His radical pair albeit via a different mechanism to the formation of the flavin-Trp radical pairs presented in the rest of this work. The interpolated average of the  $\Delta A$  spectrum of H6 recorded at  $t = 100 \mu s$  and the  $\Delta\Delta A$  spectrum recorded at  $t = 1 \mu s$  is used as reference spectrum for FH• in the spectral deconvolution described in the main text. Note that no significant  $\Delta\Delta A$  is observed at wavelengths above 650 nm despite a large  $\Delta A$  signal in that wavelength range. This is consistent with the assumption that the MFE originates in a spin-correlated flavin-His radical pair and that the concentration of  $^3F^*$  is independent of the applied magnetic field.

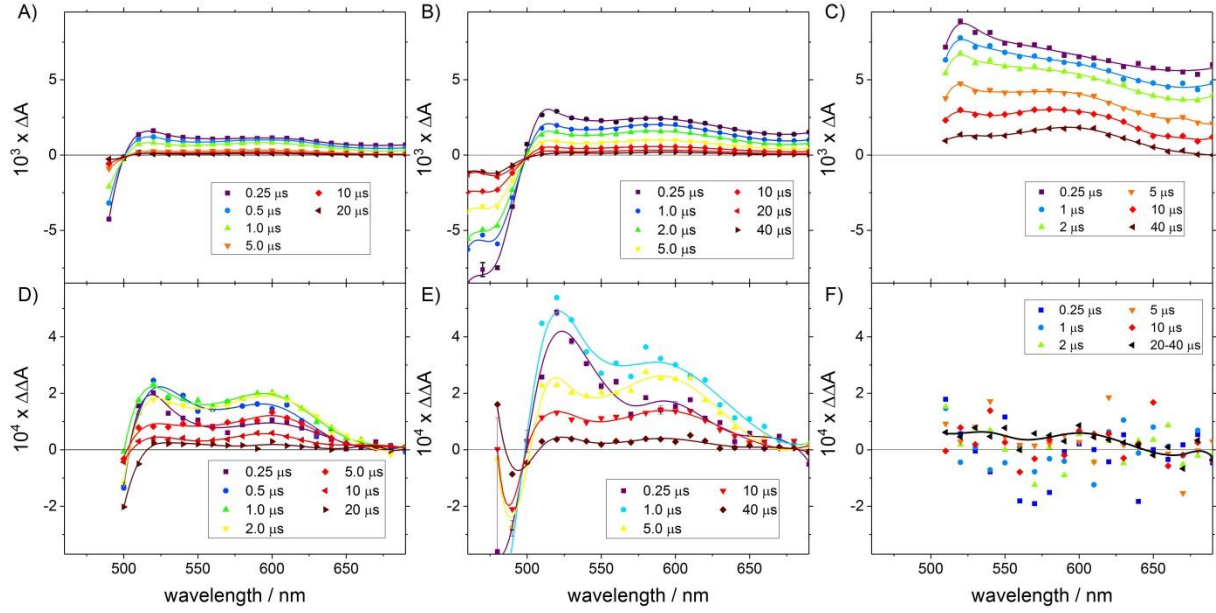
### (c) W13, W16, and W20 maquettes

Figure S4A, B and C show  $\Delta A$  spectra measured at various PPD times for W13, W16, and W20 respectively. These data and their time-dependence can be understood using the spectra of  $^3F^*$ , FH•,  $F^{\bullet-}$  and W• that have either been measured in this work or are available from the literature (see Figure 4). The initially formed tryptophan radical cation, WH•<sup>+</sup>, rapidly

deprotonates and is not observed. The details of the spectral deconvolution are given below. Generally, the bleaching of the flavin ground state is observed as a negative contribution to  $\Delta A$  below 520 nm and the absorption between 520 and 640 nm is dominated by  $^3F^*$ ,  $FH^\bullet$ ,  $F^{\bullet-}$  and  $W^\bullet$ . Only  $^3F^*$  absorbs significantly at wavelengths  $> 650$  nm. This is reflected in the absence of  $\Delta\Delta A$  signal at wavelengths  $> 650$  nm despite strong  $\Delta A$  signals (see Figure S4A-C, for W13, W16, and W20 respectively). The shape of the  $\Delta\Delta A$  spectra reflects the absorption profiles of the flavin and Trp radicals ( $FH^\bullet$ ,  $F^{\bullet-}$ , and  $W^\bullet$ , see Figure 4). This is consistent with the assumption that the magnetic field effect originates in a spin-correlated flavin-tryptophan radical pair and, once again, that the quantum yield of  $^3F^*$  is not sensitive to magnetic fields.



**Figure S4a.**  $\Delta A$  spectra of ca. 20  $\mu M$  flavomaquette (A) W13, (B) W16, and (C) W20 in pH 6.5 phosphate buffer taken at various PPD times. (D), (E), and (F) show the respective  $\Delta\Delta A$  spectra. The black triangles in (F) show the average  $\Delta\Delta A$  spectra measured at 20 and 40  $\mu s$  PPD. Solid lines in all six panels are spline fits to guide the eye. In (F), the solid line is the fit to the average  $\Delta\Delta A$  measured at 20 and 40  $\mu s$  PPD. See also Figure S4b.



**Figure S4b.** The same data as in Figure S4a, plotted with common  $\Delta A$  (A-C) and  $\Delta\Delta A$  scales (D-F) to allow an easier comparison of the relative amplitudes of the signals.

#### (d) Spectral deconvolution

$\Delta A$  spectra of W20, W16, W13 and the control maquette (see Figures S5A, B, C, and D, respectively) were fit to reference spectra (see Figure 4A) using a least squares fitting routine (The MathWorks, MATLAB R2014b) and the following fit function,

$$S(\lambda, t) = \sum_i c_i(t) S_i(\lambda) \quad (1)$$

where  $S_i(\lambda)$  is the normalized reference spectrum for species  $i$  ( $i = {}^3\text{F}^*$ ,  $\text{FH}^\bullet$ ,  $\text{F}^{\bullet-}$ ,  $\text{W}^\bullet$ ), and  $c_i(t)$  is the corresponding amplitude. The reference spectra were normalized to give an integrated absorbance of 1 so that  $c_i(t)$  represents the relative contribution of species  $i$  at time  $t$ .<sup>a</sup> The fitting was repeated for all PPD times to obtain the time-dependence shown in Figure S5 for the four maquettes.  ${}^3\text{F}^*$  absorbs strongly in the observed wavelength region and contributes the most to the overall absorbance at early PPD times in all four cases. The species  $\text{F}^{\bullet-}$  and  $\text{W}^\bullet$

<sup>a</sup> N.B.  $\sum_i c_i(t)$  is the absorbance,  $S(\lambda, t)$ , integrated over the wavelength range of the measurement.



absorb weakly and contribute comparatively little. For W20 the spectra are dominated by an exponentially decaying absorption of  $^3F^*$  and an almost constant contribution from  $FH^\bullet$ . W16 and W13 both show a significant contribution from  $F^{\bullet-}$ ,  $^3F^*$ , and  $FH^\bullet$  at early PPD times. For both W16 and W13, the  $F^{\bullet-}$  signal decays within 10  $\mu s$  while the  $FH^\bullet$  contribution persists beyond the 40  $\mu s$  time frame of the measurement. In the control, no species other than  $^3F^*$  contributes significantly to the overall absorbance.

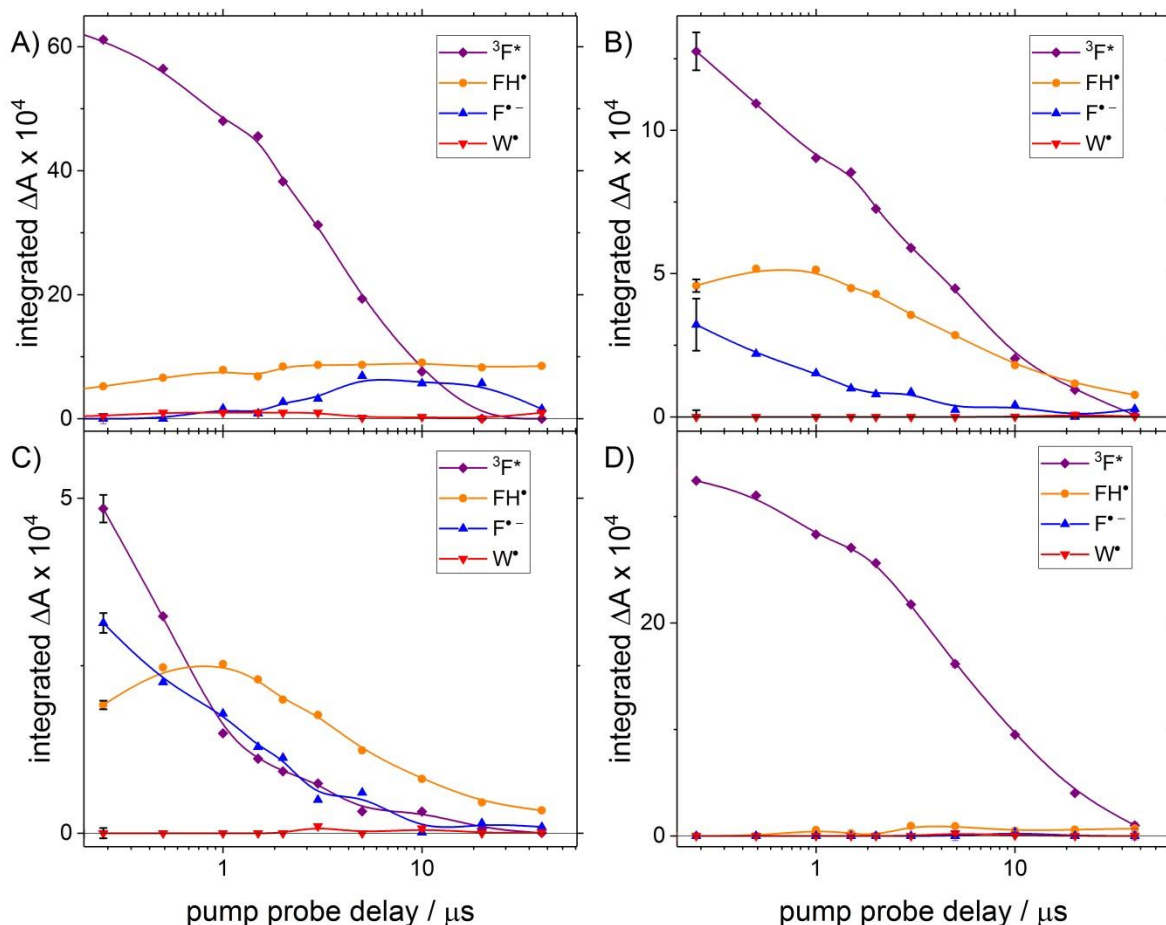


**Figure S5.** The contribution coefficients as a function of PPD time for the individual species observed for (A) W20, (B) W16, (C) W13, and (D) the control maquette. Representative uncertainties are shown for  $t = 250$  ns; those in panels (A) and (D) are smaller than the size of the symbols.

All observations are consistent with the suggested photocycle (see Scheme 1) in particular regarding the formation of a long lived  $FH^\bullet$  radical through protonation of  $F^{\bullet-}$  formed from  $^3F^*$ .

## References

- (1) Brown, S. S.; Ravishankara, A. R.; Stark, H. *J. Phys. Chem. A* **2000**, *104*, 7044-7052.
- (2) Ghisla, S.; Mayhew, S. G. *Eur. J. Biochem.* **1976**, *63*, 373-390.
- (3) Li, G. F.; Glusac, K. D. *J. Phys. Chem. A* **2008**, *112*, 4573-4583.
- (4) Bialas, C.; Jarocha, L. E.; Henbest, K. B.; Zollitsch, T. M.; Kodali, G.; Timmel, C. R.; Mackenzie, S. R.; Dutton, P. L.; Moser, C. C.; Hore, P. J. *J. Amer. Chem. Soc.* **2016**, *138*, 16584-16587.
- (5) Sakai, M.; Takahashi, H. *J. Mol. Struct.* **1996**, *379*, 9-18.
- (6) Magerl, K.; Stambolic, I.; Dick, B. *Phys. Chem. Chem. Phys.* **2017**, *19*, 10808-10819.
- (7) Tsentalovich, Y. P.; Lopez, J. J.; Hore, P. J.; Sagdeev, R. Z. *Spectrochimica Acta Part a-Molecular and Biomolecular Spectroscopy* **2002**, *58*, 2043-2050.
- (8) Huvaere, K.; Skibsted, L. H. *J. Amer. Chem. Soc.* **2009**, *131*, 8049-8060.
- (9) Muszkat, K. A.; Wismontskiknittel, T. *Biochemistry* **1985**, *24*, 5416-5421.